Contract No:

This document was prepared in conjunction with work accomplished under Contract No. DE-AC09-08SR22470 with the U.S. Department of Energy (DOE) Office of Environmental Management (EM).

Disclaimer:

This work was prepared under an agreement with and funded by the U.S. Government. Neither the U. S. Government or its employees, nor any of its contractors, subcontractors or their employees, makes any express or implied:

1) warranty or assumes any legal liability for the accuracy, completeness, or for the use or results of such use of any information, product, or process disclosed; or
2) representation that such use or results of such use would not infringe privately owned rights; or
3) endorsement or recommendation of any specifically identified commercial product, process, or service.

Any views and opinions of authors expressed in this work do not necessarily state or reflect those of the United States Government, or its contractors, or subcontractors.

SRNL
SAVANNAH RIVER NATIONAL LABORATORY
OPERATED BY SAVANNAH RIVER NUCLEAR SOLUTIONS

December 30, 2019

SRNL-STI-2019-00193
Revision 0

TO: B. T. BUTCHER, 773-42A

FROM: T. L. DANIELSON, 773-42A

REVIEWER: B. T. BUTCHER, 773-42A

PORFLOW IMPLEMENTATION OF VADOSE ZONE CONCEPTUAL MODEL FOR SLIT AND ENGINEERED TRENCHES IN THE E-AREA LOW LEVEL WASTE FACILITY PERFORMANCE ASSESSMENT

Scope

A summary of the conceptual models to be used in representing slit (ST) and engineered trenches (ET) in PORFLOW (ACRi 2018) simulations as part of the performance assessment (PA) of the E-Area Low Level Waste Facility (ELLWF) is presented. Key details that are discussed include: model geometries, spatially dependent hydro-stratigraphic representations, model dimensionality, and boundary conditions (i.e., infiltration rates, cover overhangs, subsidence). Accounting for differences in the percent of non-crushable materials, eighteen unique models, defined by seven hydro-stratigraphic groupings, will be used to represent slit and engineered trenches.

Discussion

The relevance of several hydro-stratigraphic and design features specific to the ELLWF has been evaluated using PORFLOW to assist in the development and implementation of the vadose zone conceptual models to be used in the PA. In the following subsections, a summary of these evaluations is presented to highlight the actions and decisions in the development and implementation of the proposed conceptual models.

Disposal Unit Length

The longest footprint in the ELLWF is ST1 (675.3 feet). While the length of the majority of STs and ETs fall within 3% of the length of ST1, the lengths of ST10, ST11, ST21, ST22, and ET3 are substantially different (i.e., greater than 10%, and up to 33% different). Therefore, a series of PORFLOW simulations were performed to confirm that a generic model of any length could be used to represent any trench without impacting the flux to the water table. A generic 2D model with waste uniformly distributed across 600-, 500-, 400-, 300-, 200-, and 100-foot lengths was used to calculate steady-state flow and transient transport solutions to obtain the flux to the water table for the list of nine radionuclide species investigated in Hamm et al. 2018. Because the specified quantity of the radionuclide species is the same regardless of length, and no solubility limitations are imposed, all differences in the peak flux to the water table were negligible (<~3%) and attributed to numerical dispersion. Therefore, one generic waste zone length can be used for all disposal units (DUs) in the ELLWF.

Hydro-stratigraphy

The elevations of the water table and various sub-surface hydro-stratigraphic features have been reported on a trench-by-trench basis for the ELLWF by Bagwell et al. 2017. Of interest during the development of the conceptual models are those features which will impact the radionuclide travel time through the vadose zone, such as depth to the water table and the quantity of clayey material beneath the waste zone. A 3D reconstruction (Figure 1) and contour mappings (Figure 2 through Figure 5) of the hydro-stratigraphic surfaces were created to highlight the relevant features that should be represented in the conceptual models for ETs and STs.

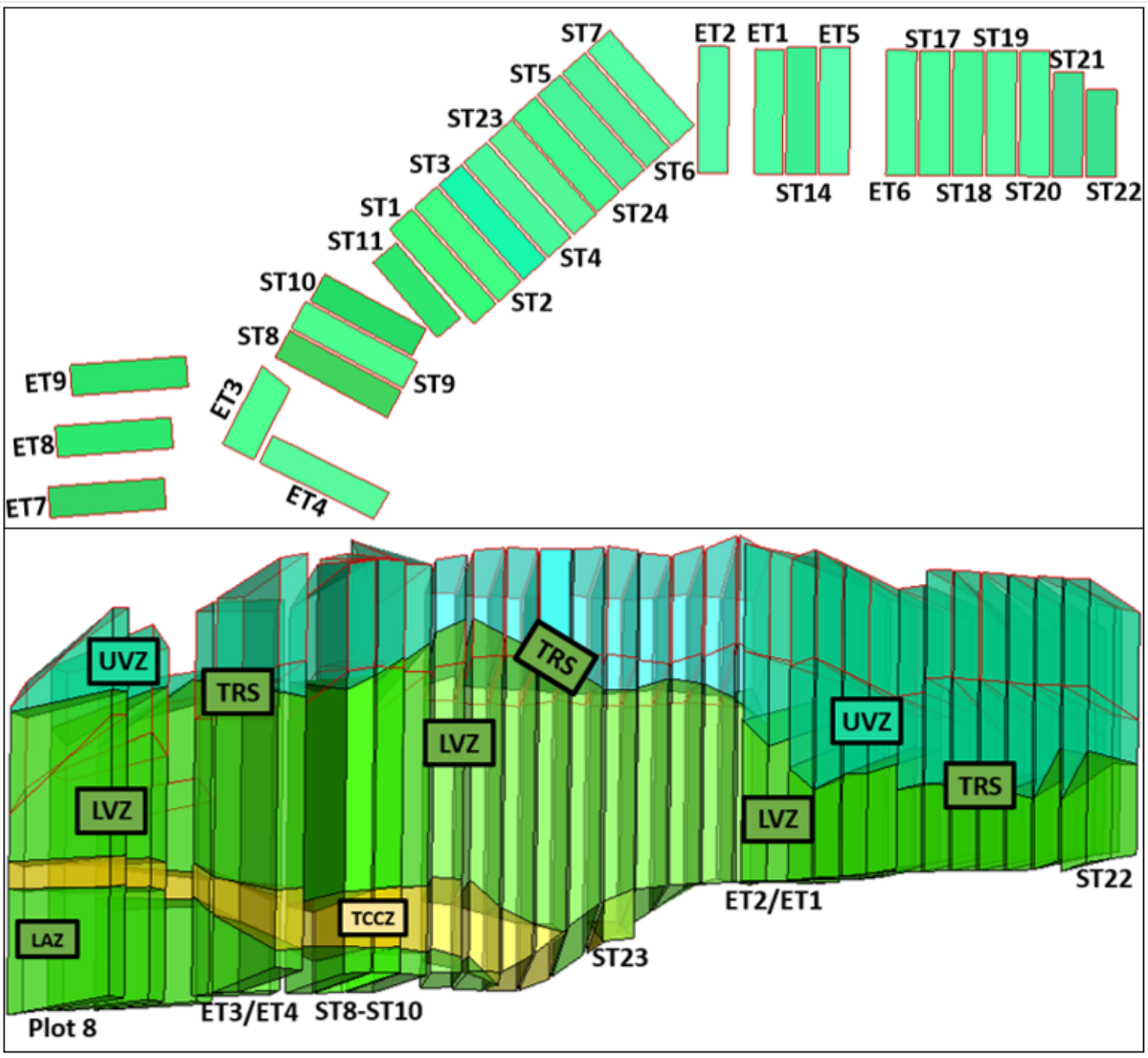

Figure 1. 3D reconstruction of hydro-stratigraphic surfaces as reported by Bagwell et al. 2017. The waste zone, which is assumed to extend 20 feet below the ground surface, is outlined in red. UVZ, TRS, LVZ, TCCZ, and LAZ, mark the upper vadose zone, tobacco road sand, lower vadose zone, tan clay confining zone, and the lower aquifer zone, respectively.

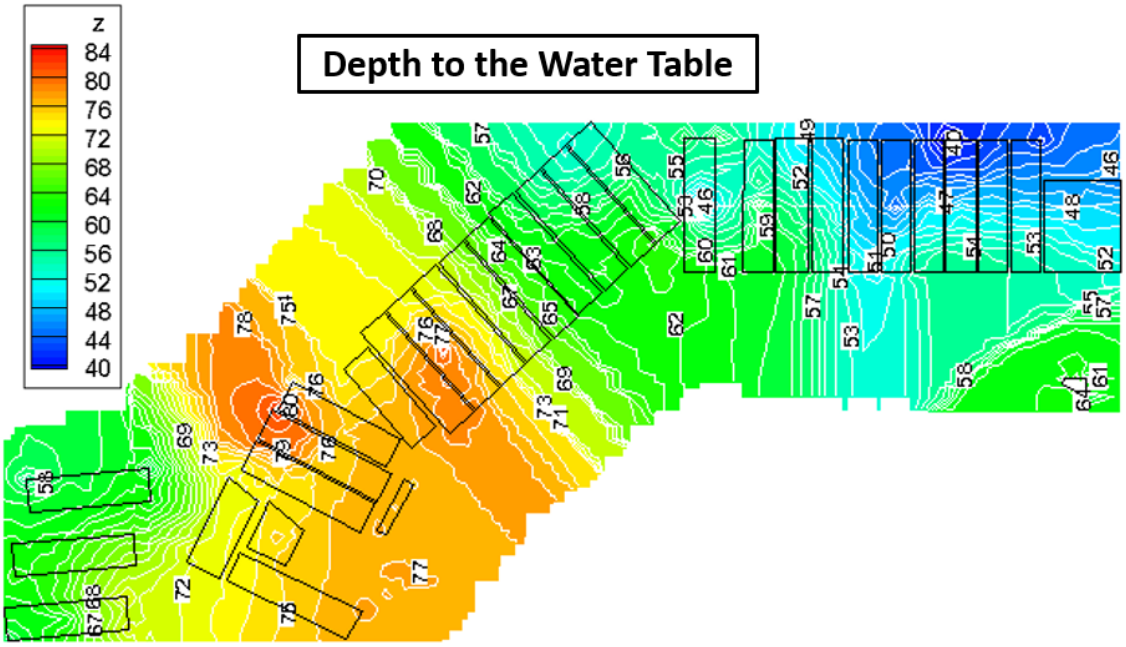

Figure 2. Depth (feet) to the water table from ground surface.

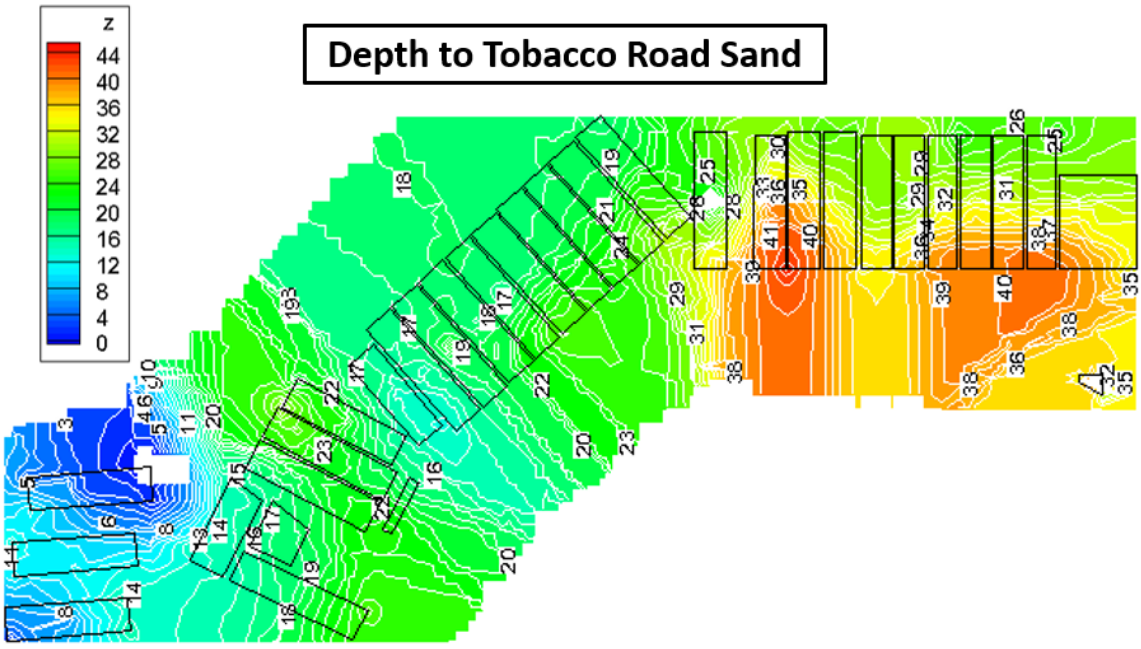

Figure 3. Depth (feet) to the tobacco road sand from ground surface.

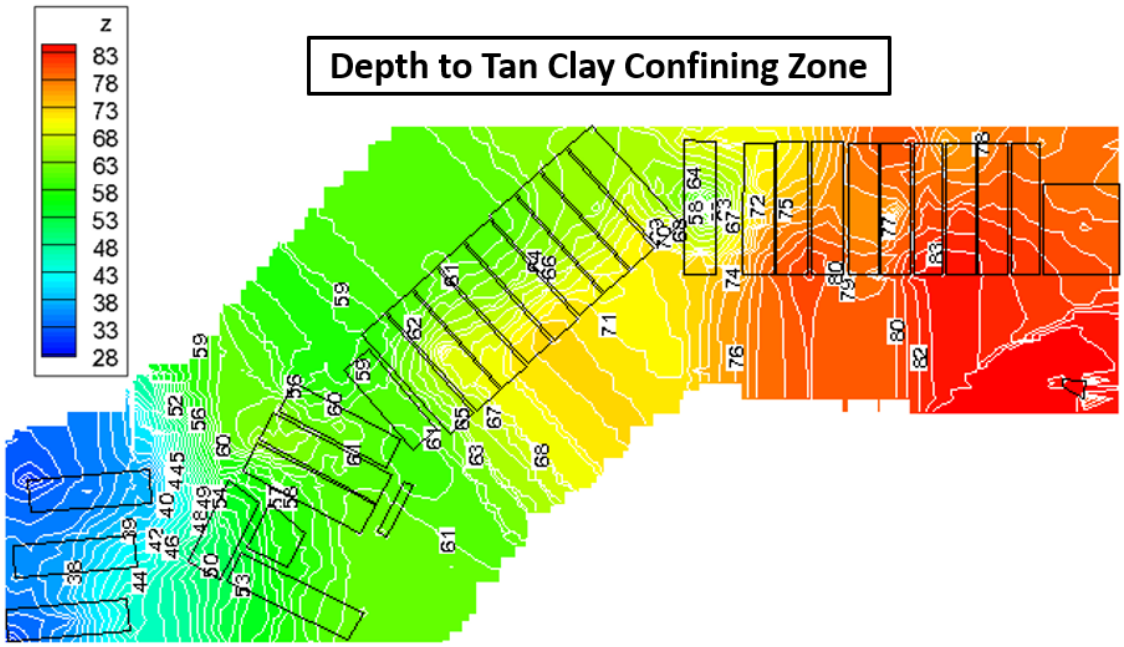

Figure 4. Depth (feet) to the tan clay confining zone from ground surface.

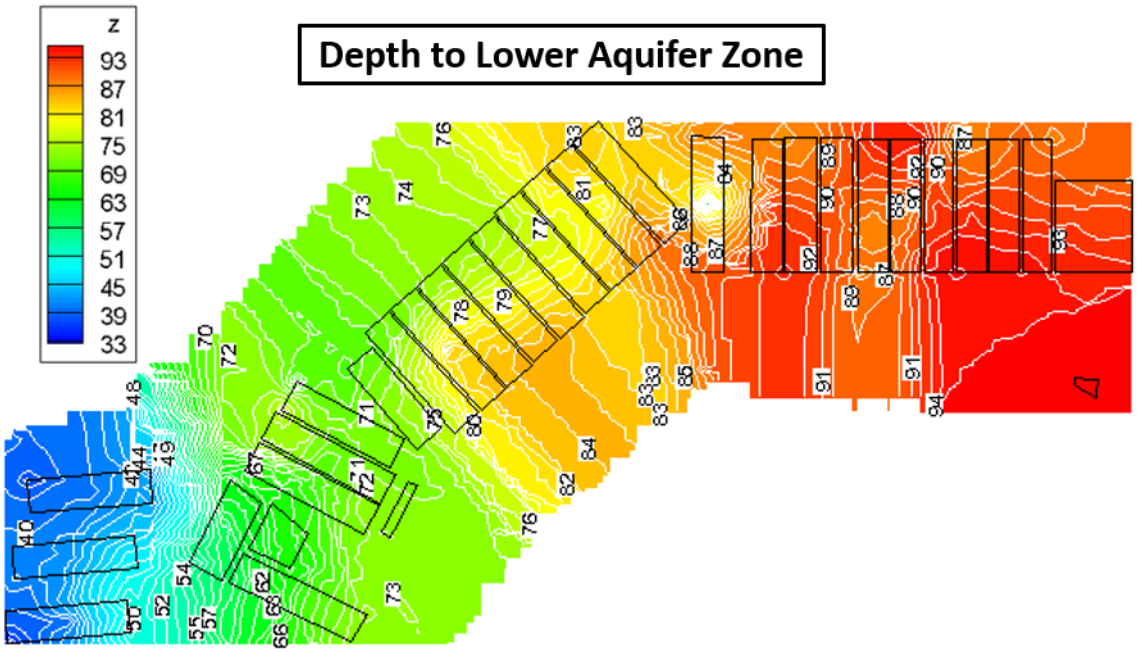

Figure 5. Depth (feet) to the lower aquifer zone from ground surface.

Inspection of the depth to the water table reveals a substantial difference moving from northeast (~80 feet from ground surface to water table) to southwest (~45 feet from ground surface to water table) of the ELLWF, and therefore, the travel time through the vadose zone can vary significantly based on location. Clayey material exists beneath every waste zone, present as either a part of the upper vadose zone (UVZ)

or the tan clay confining zone (TCCZ). The lower hydraulic conductivity of clayey material (when compared to sandy material of the lower vadose zone and lower aquifer zone), along with higher K_d's, increases travel times through the vadose zone. Figure 6 shows the range of thicknesses of clayey material beneath the waste zone(s) in the ELLWF (i.e., thickness of UVZ clayey material beneath the waste zone plus thickness of TCCZ material beneath the waste zone). The minimum and maximum thicknesses of clayey material are approximately 2 feet and 17 feet, respectively.

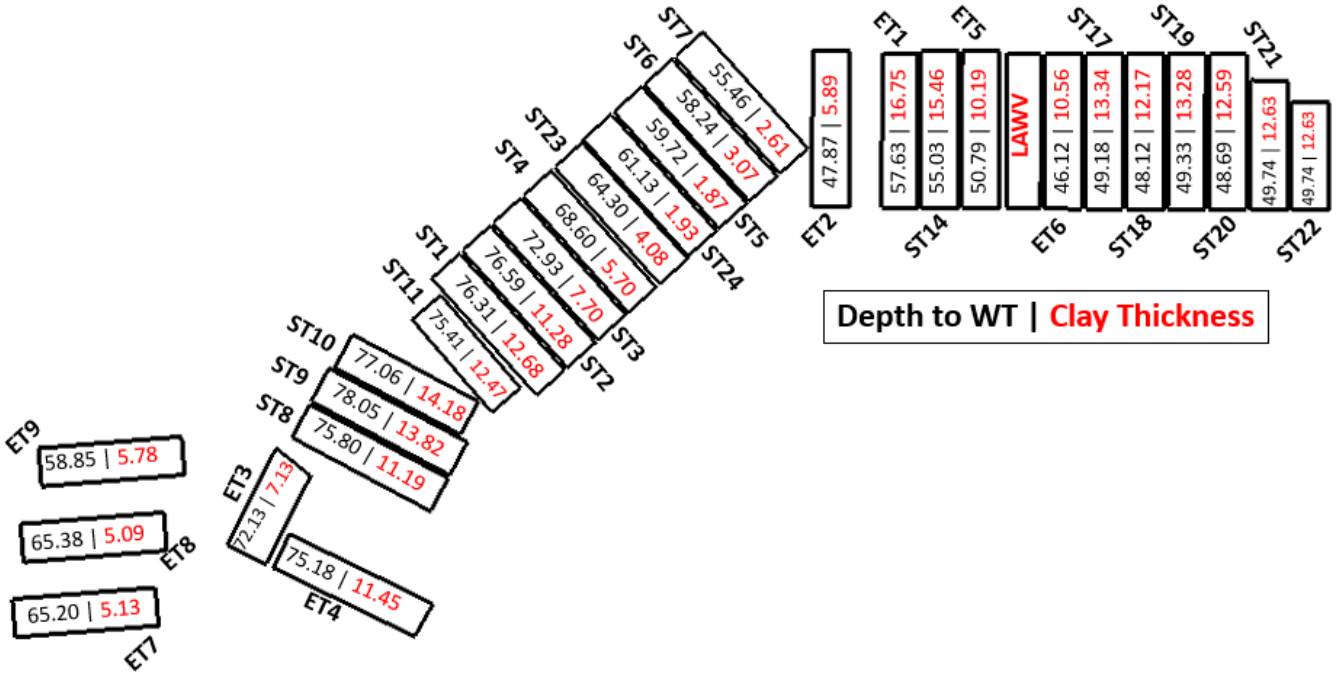

Figure 6. Depth (feet) to the water table and average thickness (feet) of the clayey material beneath the waste zone.

Additional spatially varying features include the presence of sandy versus clayey material neighboring the waste zones and the presence of the lower aquifer zone (LAZ) beneath the tan clay confining zone (TCCZ) in the northeastern section of ELLWF. By comparison, the central and southwestern portions of ELLWF have only clayey material neighboring the waste zone and only sandy material beneath the upper vadose zone.

The range of depths to the water table and clayey thicknesses beneath the waste zones require the use of multiple models to adequately represent relevant hydro-stratigraphic features while maintaining a reasonable level of conservatism. However, it is desirable to use the fewest number of models necessary to reduce overall complexity and cost associated with model development. Two approaches have been taken to reduce the overall number of models: 1) eliminating irrelevant or non-conservative features to create generic representations and 2) conservatively grouping trenches that share common hydro-stratigraphy (the final groupings are shown in Figure 21).

With regard to eliminating irrelevant or non-conservative features to create generic representations, two key features have been investigated using PORFLOW simulations: 1) vertical positioning of clayey material beneath the waste zone (Figure 7) and 2) sandy vs. clayey material neighboring the waste zone (Figure 8). A series of steady-state flow solutions with differing infiltration boundary conditions were obtained and provided as input for transient radionuclide contaminant transport through the vadose zone. The peak fluxes to the water table for nine radionuclides were obtained to inspect any relevant differences and down-select to the most conservative representation (for more information on the PORFLOW models' material properties, time discretization, boundary conditions/subsidence models, radionuclides, etc. see Hamm et al. 2018 – only the model geometries were changed).

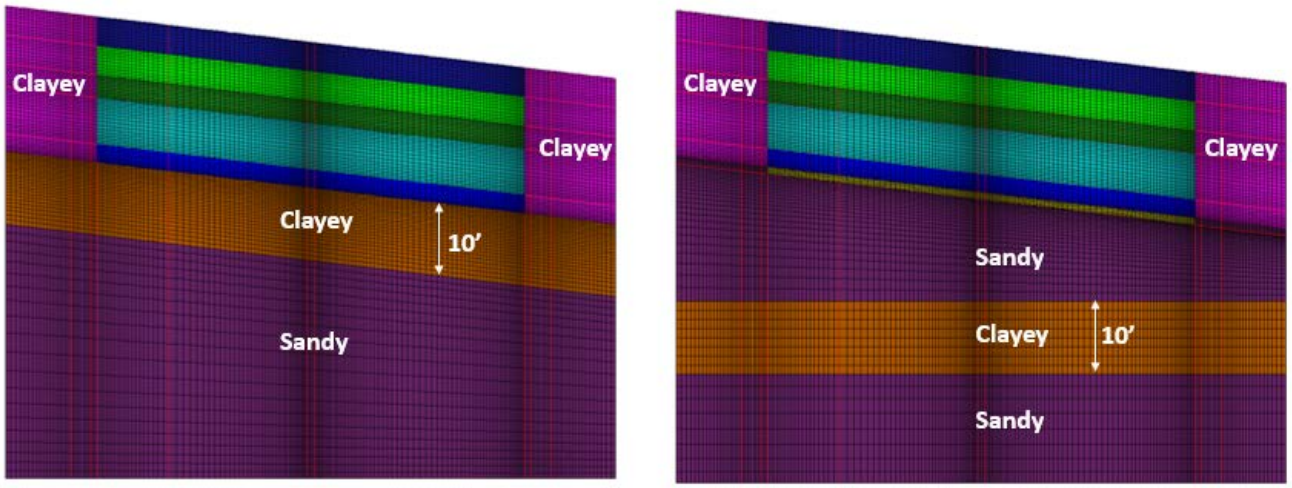

Figure 7. PORFLOW model geometries used to investigate the vertical positioning of clayey material beneath the waste zone.

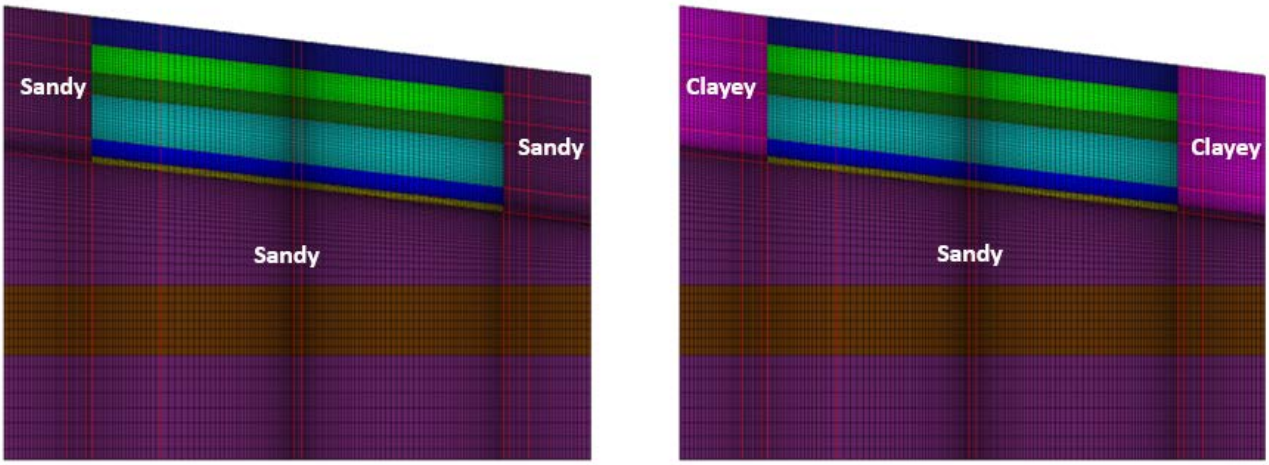

Figure 8. PORFLOW model geometries used to investigate sandy versus clayey material neighboring the waste zone.

The vertical positioning of the clayey material beneath the waste zone was found to have no impact on the flux to the water table. This suggests that it is reasonable to use a generic clayey material beneath the waste zone with a thickness corresponding to the sum of TCCZ thickness and UVZ thickness, with the assumption that the material properties are the same. Comparing sandy versus clayey material neighboring the waste zone, negligible difference in the overall peak flux to the water table was found, however, slightly higher concentrations through time are noticed when clayey material neighbors the waste zone, as shown for three radionuclides in Figure 9. This result suggests clayey material neighboring the waste zone is conservative. Based on these investigations, it is concluded that the depth to the water table and the thickness of the clayey material beneath the waste zone are the two primary considerations for creating conceptual models that represent groups of DUs in ELLWF.

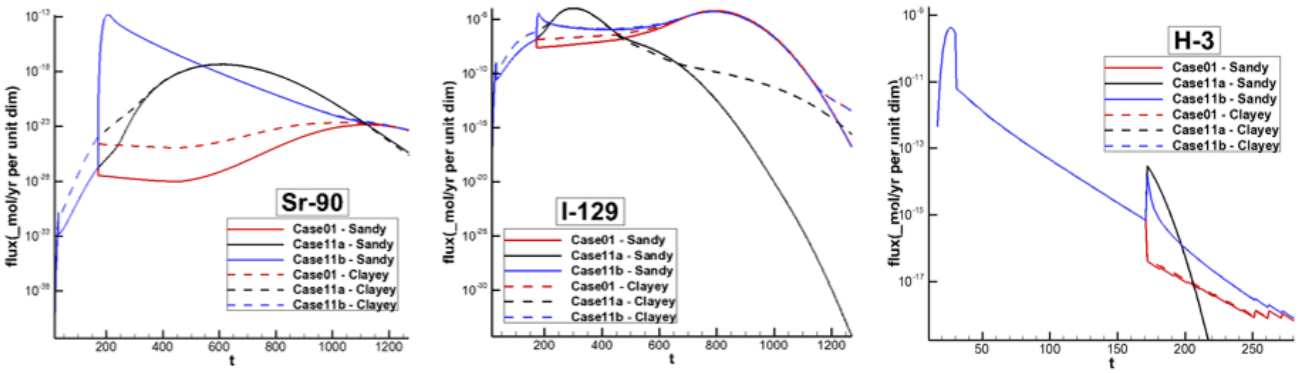

Figure 9. Flux to the water table for Sr-90, I-129, and H-3 comparing sandy and clayey material neighboring the waste zone.

Model Dimensionality

A preliminary analysis was performed to compare 2-dimensional and 3-dimensional model geometries and understand if a 2-dimensional model sufficiently represents asymmetrical features such as discrete subsided holes. In previous work (Hamm et al. 2018), the discrete hole was represented by a 12-foot-wide section in the center of the disposal unit. Translating the 2D representation to 3D, the 12-foot hole is shown by the dotted rectangle in the center of the disposal unit in Figure 11. A discrete region that represents 2% subsidence can also be defined by a 46' x 46' square, as shown by the solid outlined squares in Figure 11. Case01 and Case11a (from Hamm et al. 2018) translate directly from 2D to 3D, except for corner units (e.g., ET3, ET4, ST22), where boundary conditions are applied across different regions of the top of the model. For the generic 3D models that are described in the current section below, only the model geometry has changed – material properties, time discretization, radionuclide properties, etc. are the same as those in Hamm et al. 2018.

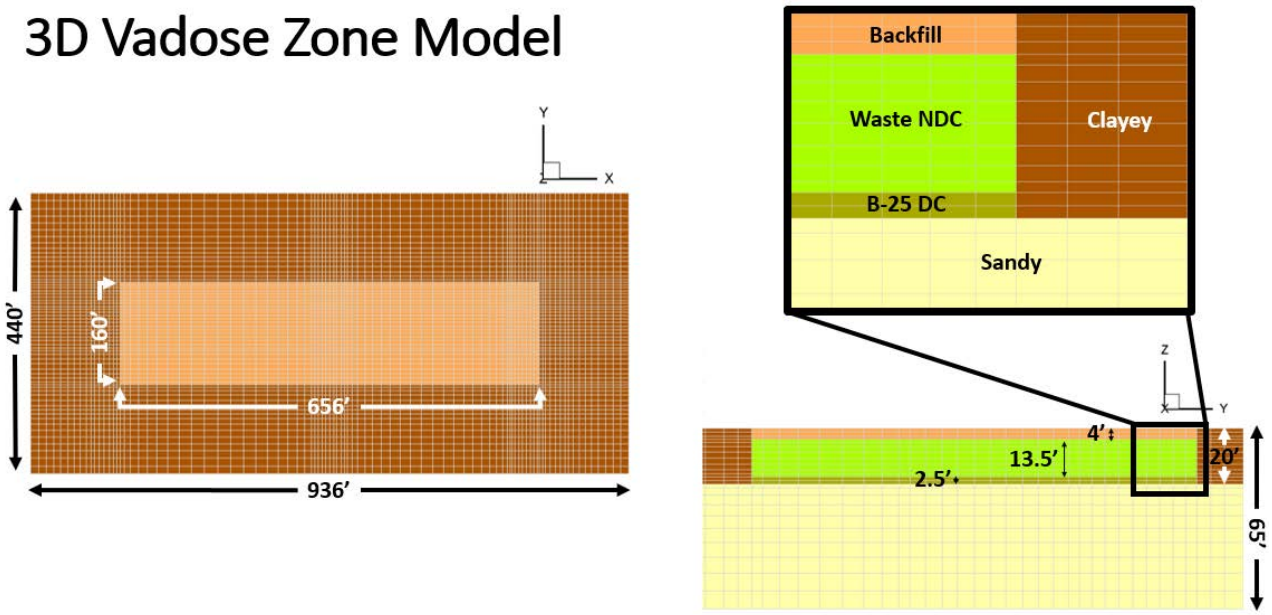

Figure 10. 3D vadose zone model for a disposal unit that is 65 feet from the water table. The 2D cross-section matches the cross section in the bottom right corner.

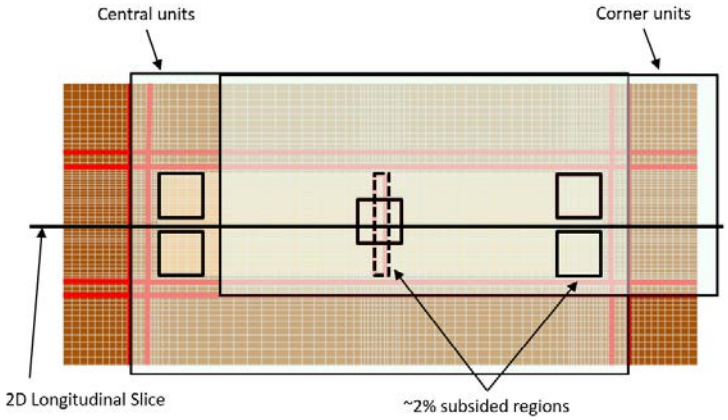

Figure 11. Various subsidence hole shapes and locations for the 3D model. Red lines mark the 10-foot and 40-foot cover overhangs for the interim and final cover.

Comparing the fluxes to the water table resulting from the 2D model to the 3D analogue (center and corner cases with a 12-foot hole representing Case11b from Hamm et al. 2018), Figure 12 through Figure 15 show that there is very little difference between the central and corner units (only select radionuclides with short/long half-lives and high/low K_d's are shown). For these cases, 2D is shown to be generally conservative since the absolute peak is highest. Therefore, sources of asymmetry related to the DU's location in ELLWF can be conservatively simplified to 2D.

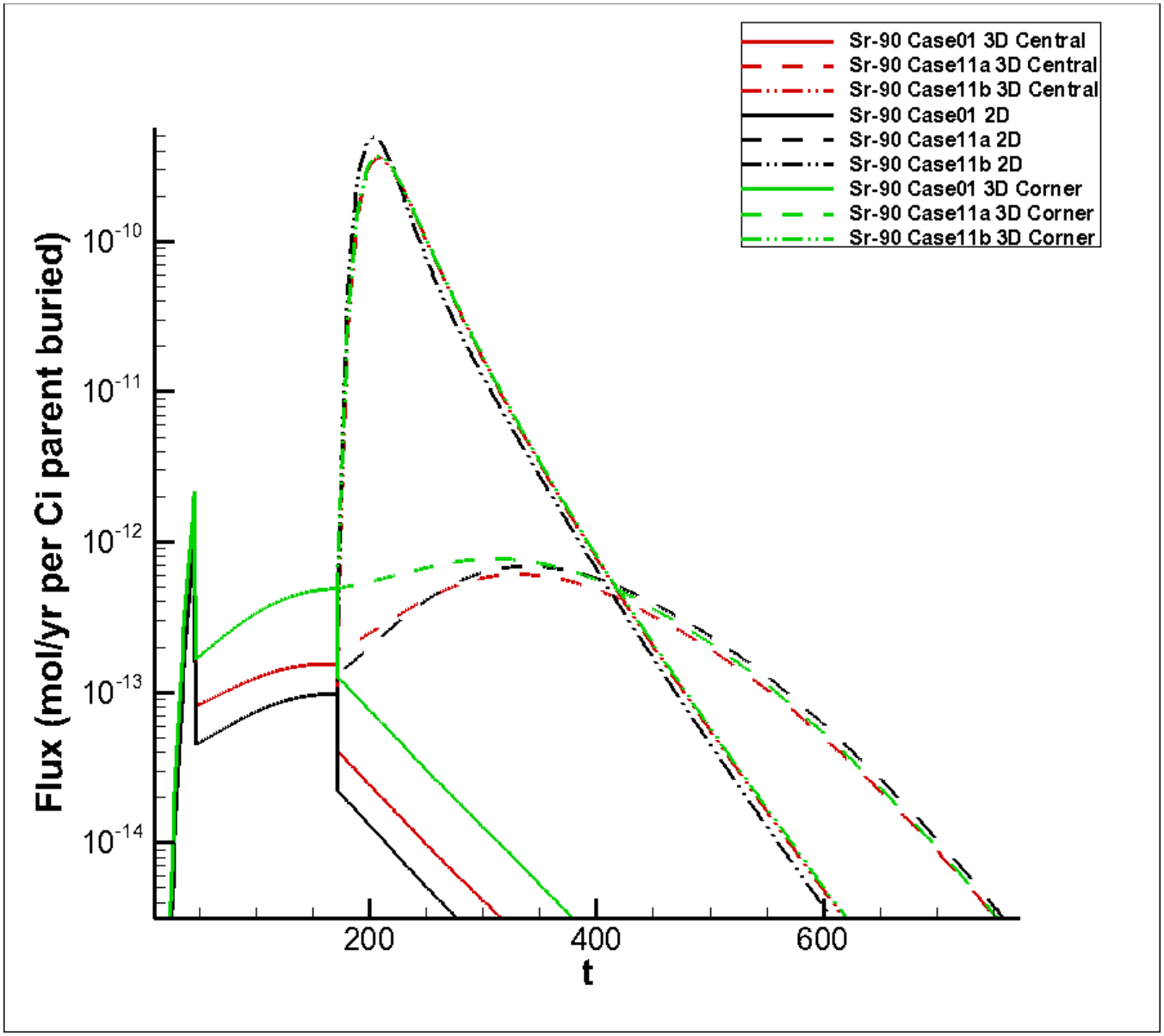

Figure 12. Sr-90 (half-life: 28.9 years; Sandy K_d: 5; Clayey K_d: 17) flux to the water table comparison between 2D longitudinal slice, 3D central unit model, and 3D corner unit model. 2D longitudinal peak is 33% higher than central and corner unit models are within 3% of each other.

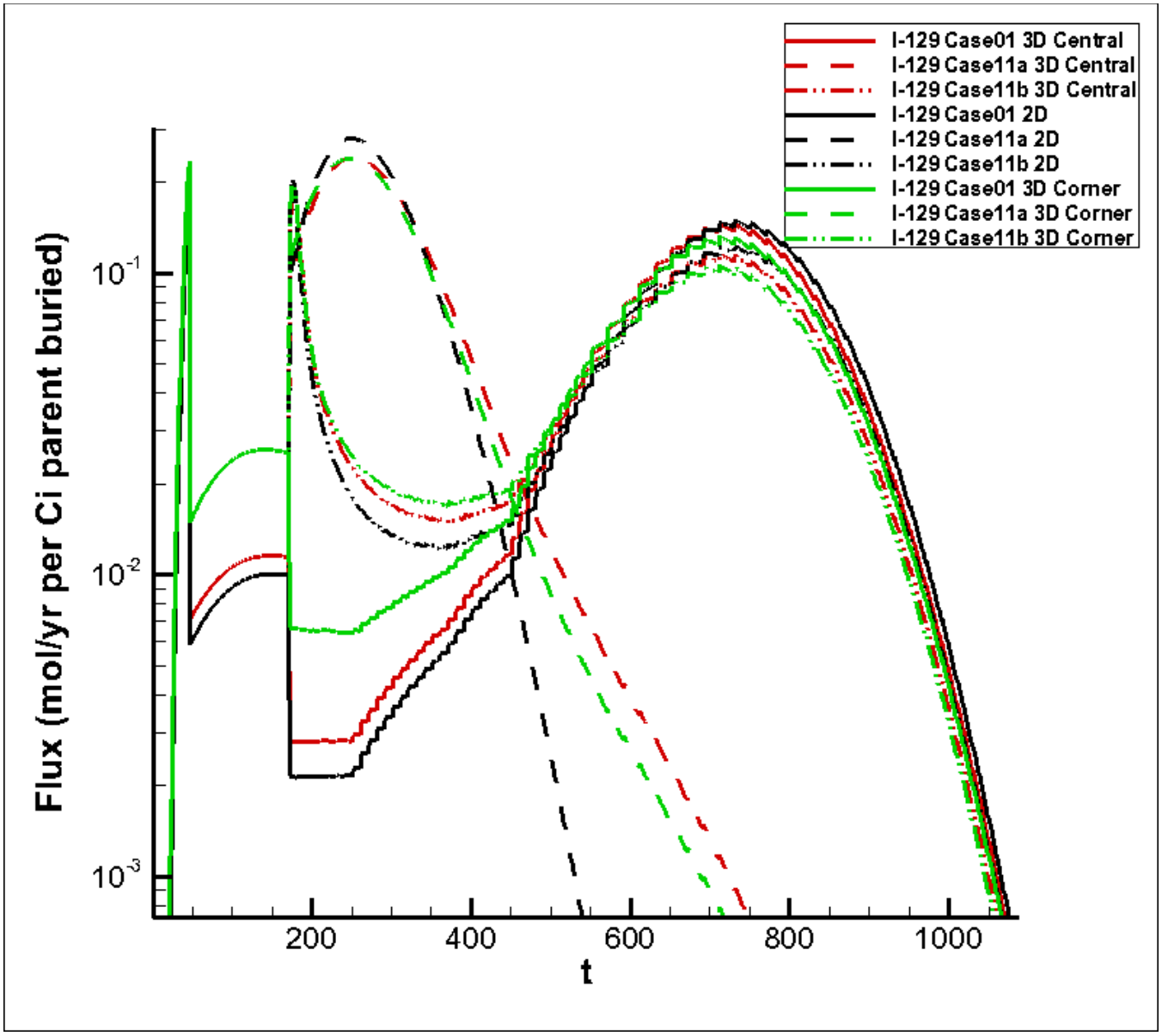

Figure 13. I-129 (half-life: 1.57e7 years; Sandy K_d: 1; Clayey K_d: 3) flux to the water table comparison between 2D longitudinal slice, 3D central unit model, and 3D corner unit model. 2D longitudinal peak is 15% higher than central and corner unit models.

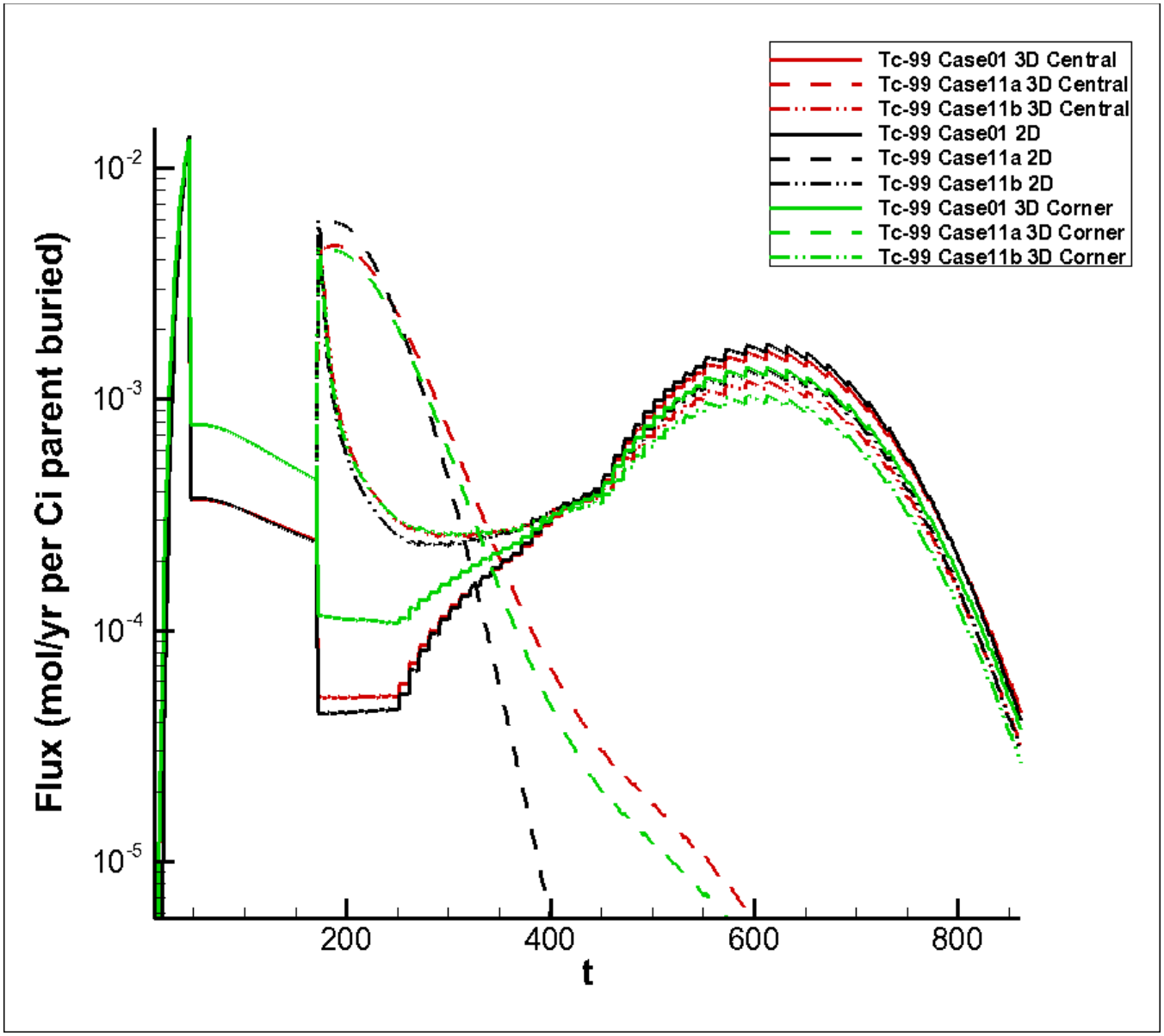

Figure 14. Tc-99 (half-life: 2.111e5 years; Sandy K_d: 0.6; Clayey K_d: 1.8) flux to the water table comparison between 2D longitudinal slice, 3D central unit model, and 3D corner unit model. Absolute peak of all three models is within 3% and the 2D model has the highest secondary peak by 25%.

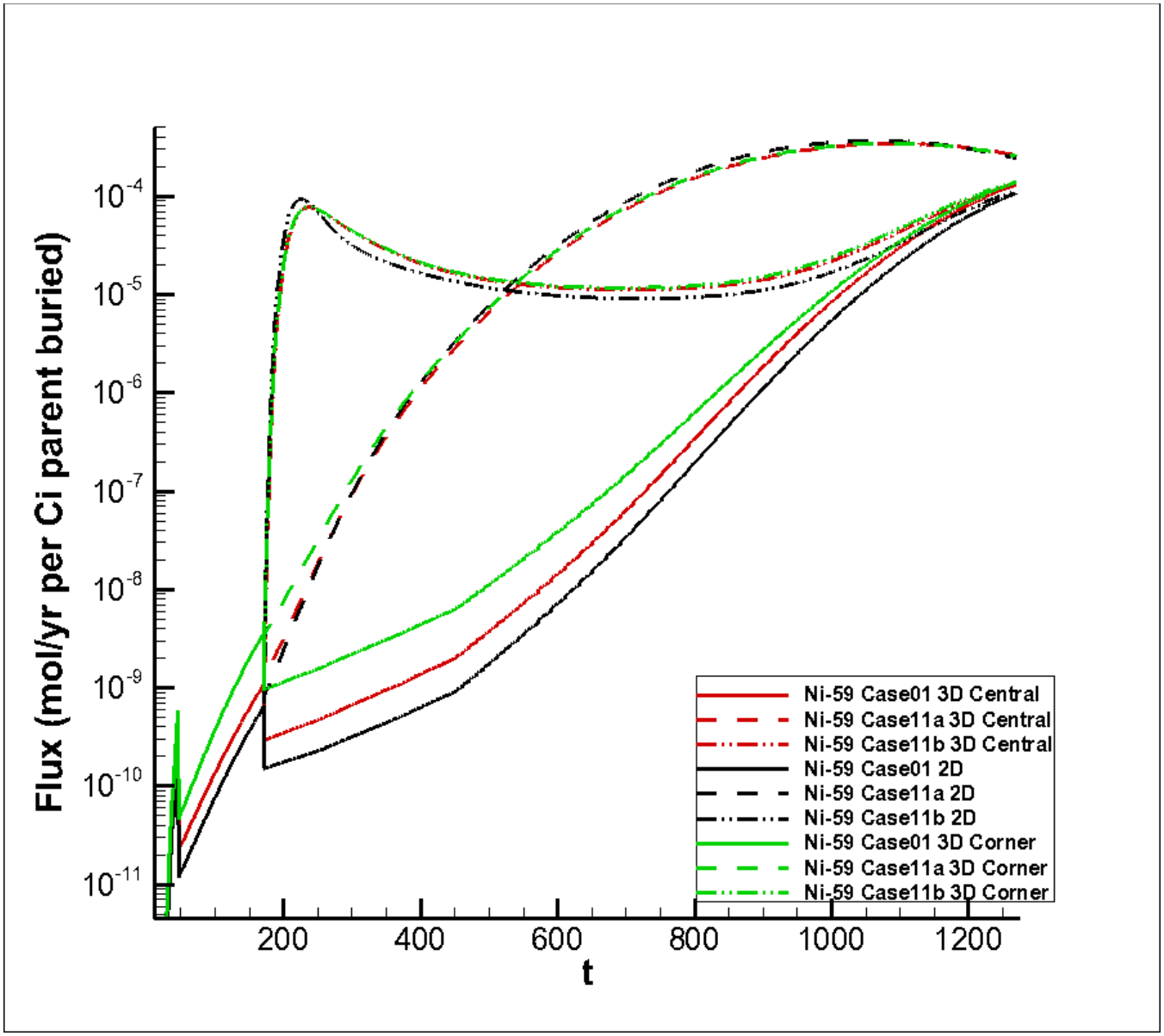

Figure 15. Ni-59 (half-life: 76000 years; Sandy K_d: 7; Clayey K_d: 30) flux to the water table comparison between 2D longitudinal slice, 3D central unit model, and 3D corner unit model. 2D peak is 20% higher than central and corner unit models.

A set of asymmetric subsidence cases (Table 1) for the discrete hole, Case11b, have been compared to the 2D model and the 3D model discussed previously. Figure 16 shows that the peak flux to the water table for the asymmetric discrete hole subsidence cases are substantially greater than the 2D case and 3D central 12-foot hole case. This result substantiates the use of 3-dimensions so that asymmetries in subsidence models can be accounted for properly, especially since the overall increase in computational load is negligible.

Table 1. Description of asymmetric Case11b cases.

Case	*Description*
Case11b1	*46-foot x 46-foot hole in center of central disposal unit*
Case11b2	*46-foot x 46-foot hole in center of corner disposal unit*
Case11b3	*46-foot x 46-foot hole in top right corner of central disposal unit*
Case11b4	*46-foot x 46-foot hole in bottom right corner of corner disposal unit*
Case11b5	*46-foot x 46-foot hole in bottom left corner of corner disposal unit*
Case11b6	*46-foot x 46-foot hole in top left corner of corner disposal unit*
Case11b7	*46-foot x 46-foot hole in top right corner of corner disposal unit*

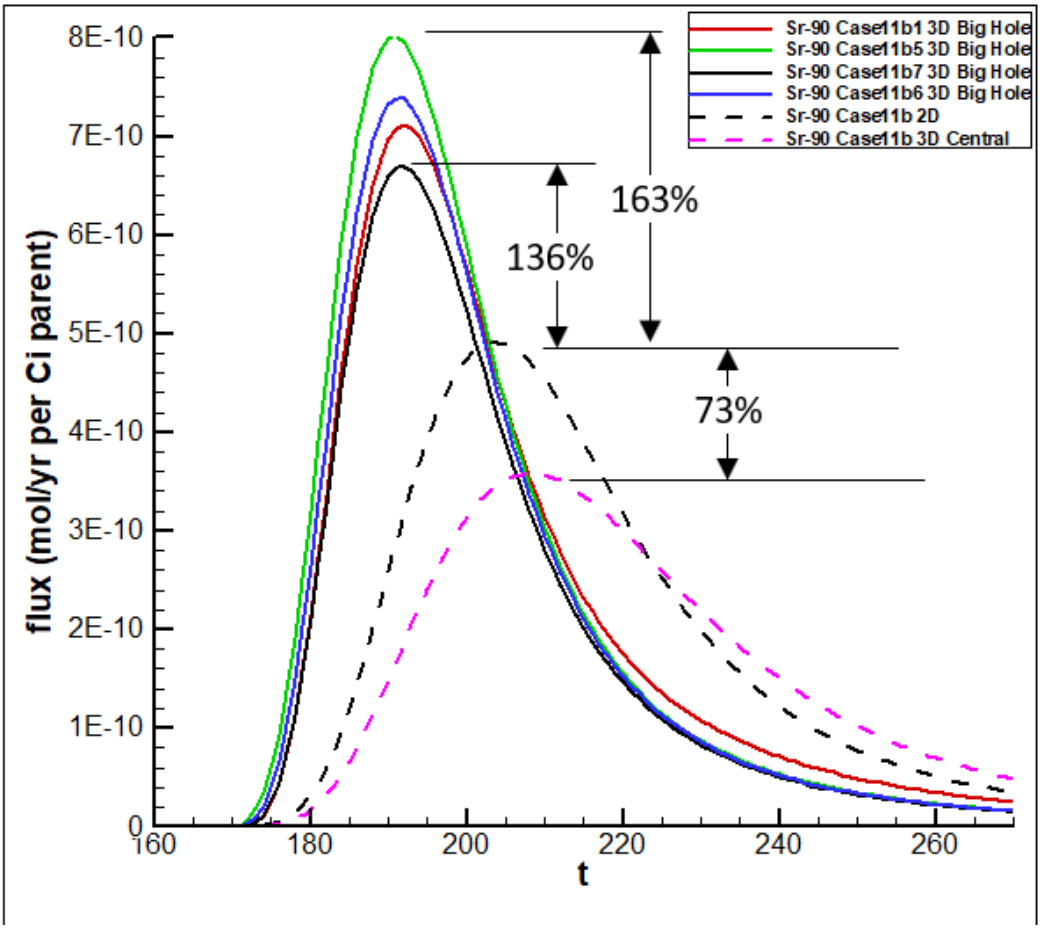

Figure 16. Sr-90 flux to the water table for various discrete hole cases where the peak fluxes are substantially different.

Trench Specific Features in 3D Models

Along with accounting for the asymmetrical model features that were presented in the previous section, 3D trench models allow for a more detailed implementation of features specific to STs and ETs. For example, in previous 2D model implementations (such as Hamm et al. 2018), a longitudinal cross-section

was used because infiltration boundary conditions for the bounding infiltration model are most appropriately represented along the longitudinal axis. However, such a representation is not capable of accounting for differences in the ET and ST geometry (i.e., one 157 ft x 656 ft trench for ETs vs. five 20 ft x 656 ft trench segments for STs). While there are benefits to a generic model representation (e.g., using the ET geometry for both STs and ETs), it is preferable to avoid introducing overly conservative assumptions when it can be readily avoided. Several tests have been performed to compare trench models implemented using the ET geometry and the ST geometry under intact and subsidence conditions. These tests are detailed in SRNL-STI-2019-00637 and SRNL-STI-2019-00750, which ultimately conclude that ET/ST-specific geometric features should be included on a trench-by-trench basis.

To avoid introducing numerical differences between models for ETs and STs, the spatial discretization along the *X* and *Y* directions of the mesh is the same for all models. Variations along the *Z* direction occur only to account for differences in the depth to the water table and clayey thickness, but the discretization of the trench is always the same. Therefore, the only difference between the ET and ST models for a particular hydro-stratigraphic grouping are the assignments of material types within regions of the mesh corresponding to the disposal unit. More specifically, ETs have uniformly specified waste across the entire DU footprint that corresponds to boxed waste (16-feet-tall before dynamic compaction and 2.5-feet-tall after dynamic compaction). STs, on the other hand, have a 10-foot-wide section of upper vadose zone material separating each of the five trench segments and 8.5-foot-wide sections of upper vadose zone material separating trench segments 1 and 5 from the edge of the overall footprint. Additionally, the waste form for STs is assumed to be hybrid waste (16-feet-tall before dynamic compaction and 8.87-feet-tall after dynamic compaction). The ST and ET models are shown in Figure 17 and Figure 18, respectively.

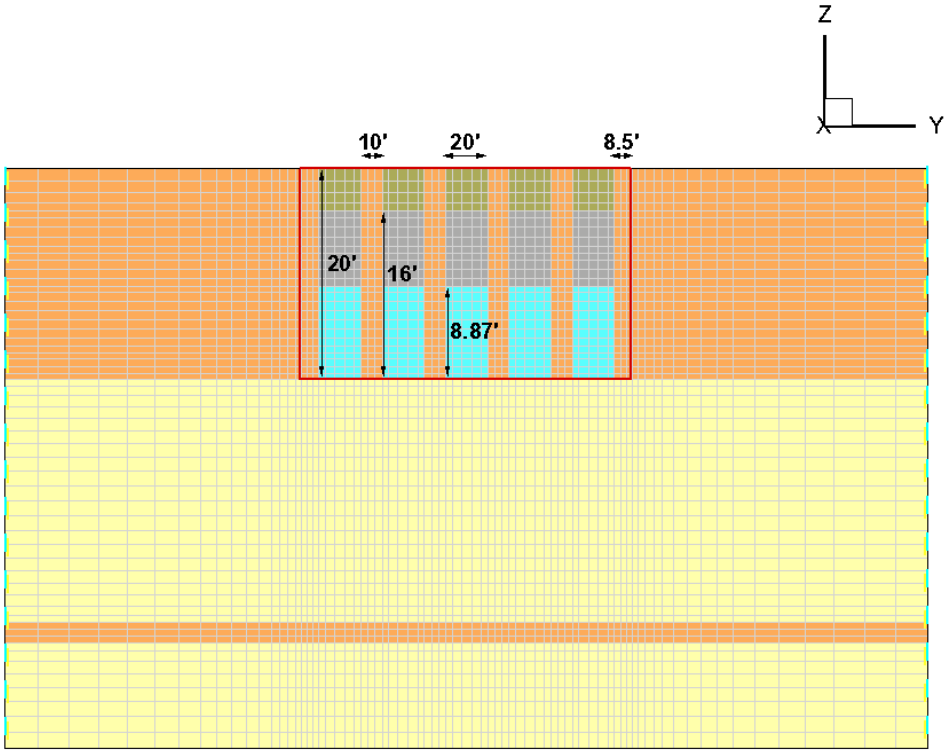

Figure 17. Cross-section of the ST model.

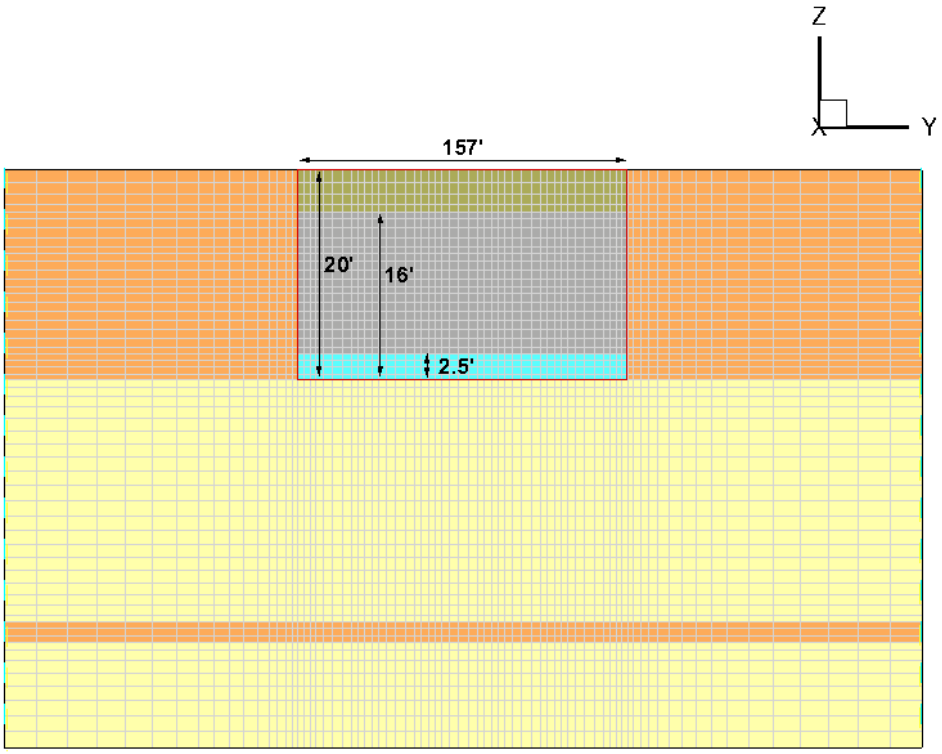

Figure 18. Cross-section of the ET model.

Infiltration Boundary Conditions

The boundary conditions of the PORFLOW models are defined by time dependent infiltration rates to account for operational time periods (uncovered), institutional control periods (interim cover), and the end of institutional control (final cover) and beyond (degradation of the final cover). Dyer et al. has performed several studies to identify bounding conceptual infiltration models pertaining to the final closure cap and provide intact and subsided infiltration estimates based on the non-crushable materials in each disposal unit. This work is summarized in the 2019 Infiltration Data Package for the ELLWF (Dyer, 2019). Each unique percent subsidence requires a separate model setup for boundary condition specification. Additionally, if a trench falls along a corner of the final closure cap (e.g., ET3 or ST22) it requires a separate model so that so that boundary conditions can be applied as shown in Figure 11 for central vs. corner units. The final cover overhangs the trench by 40 feet and the interim cover overhangs the trench by 10 feet. The operational cover that is applied to STs four years after the placement of the last waste package has the same overhang and infiltration rate as the interim cover.

Except for trenches that are known to never contain non-crushable containers, all trench models will include intact and subsided cases. Subsidence cases will be investigated using only discrete holes with a specific dimension and location. The dimensions have been selected according to the relevant geometric features so that it is possible to obtain one-to-one comparisons whether the ET or ST geometry is used. More specifically, the hole length is bounded in one direction at 20 feet (i.e., the width of a slit trench segment). The dimension along the longitudinal direction of the trench is computed based on the percent

subsidence scenario and rounded to the nearest whole number that can be accommodated by the spatial discretization of the mesh. The discrete hole sizes for each percent subsidence are provided in Table 2.

Table 2. Dimensions of discrete subsided holes for each percent subsidence case. Two lengths are necessary for the 0.54 percent subsided case due to non-uniform spatial discretization along the edge of the trench.

Percent Subsided	Subsided Area	Length	Width	Model Length
0.54	556.16	27.81	20	29.87/28
2	2059.84	102.99	20	100
3.6	3707.71	185.39	20	184
4.9	5046.61	252.33	20	252

The placement of subsided holes has been investigated in several studies summarized in SRNL-STI-2019-00750, SRNL-STI-2019-00636, SRNL-STI-2019-00637, and SRNL-STI-2019-00440. For centrally located units, six discrete hole locations are to be used and for corner units, nine discrete hole locations are to be used. Figure 19 and Figure 20 show the specific locations of each hole whose lengths are adjusted on a percent-subsidence-case basis according to Table 2.

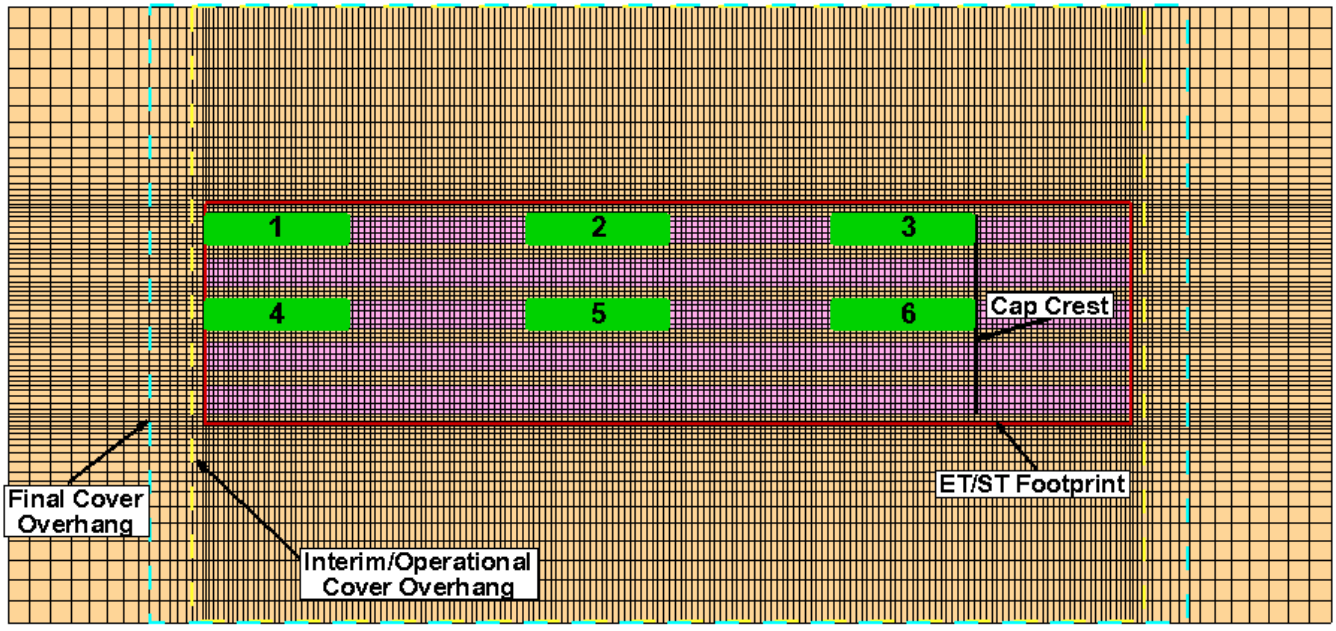

Figure 19. Discrete hole locations for centrally located ST/ETs.

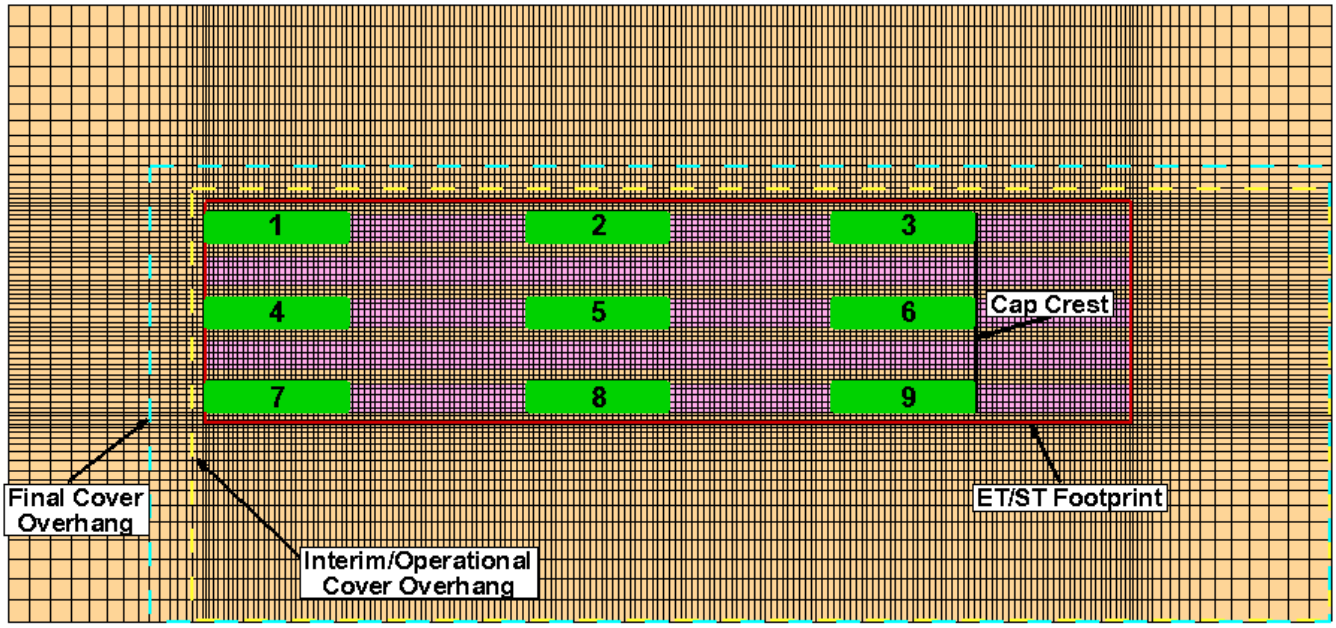

Figure 20. Discrete hole locations for ST/ETs in corner portions of the final closure cap.

Holes 1, 4, and 7 are all placed with their left edge at the end of the trench. Holes 2, 5, and 8 are each placed with their right edge at the midpoint of the trench. Holes 3, 6, and 9 are all placed with their right edge at the cap crest, which corresponds to 544 feet from the left edge of the trench using the generalized spatial discretization. The infiltration rates for each percent subsidence case and each hole location are calculated using the relationship:

$$I_S = I_B + \frac{L_U}{L_H}(I_B - I_I)$$

where I_I is the intact infiltration rate, L_U is the length of the intact upslope area, L_H is the length of the subsided region (both lengths are measured in the direction parallel to surface runoff), and I_B is the closure-cap-specific subsidence scenario background infiltration rate (i.e., annual-average rainfall minus annual-average evapotranspiration), which is 16.5 inches per year in the current work. The infiltration rates are provided in Table 3 through Table 6. The flux to the water table profile for each hole location will be blended according to the prescribed methodology discussed in SRNL-STI-2019-00440 for each disposal unit.

Table 3. Infiltration rates for 0.54% subsidence cases.

		Holes 1, 4, 7 End Position	Holes 2, 5, 8 Trench Midpoint	Holes 3, 6, 9 Crest Position
Time (yr)	Intact (in/yr)	29.87 ft long hole (in/yr)	28 ft long hole (in/yr)	28 ft long hole (in/yr)
100	0.0008	101.33	52.14	16.50
180	0.007	101.30	52.12	16.50
290	0.16	100.51	51.79	16.50
300	0.18	100.41	51.75	16.50
340	0.3	99.79	51.49	16.50
380	0.38	99.38	51.32	16.50
480	1.39	94.19	49.14	16.50
660	3.23	84.73	45.16	16.50
1100	6.82	66.27	37.41	16.50
1900	10.24	48.68	30.02	16.50
2723	11.1	44.26	28.16	16.50
3300	11.18	43.85	27.99	16.50
5700	11.3	43.24	27.73	16.50
10100	11.35	42.98	27.62	16.50

Table 4. Infiltration rates for 2% subsidence cases.

		Holes 1, 4, 7 End Position	Holes 2, 5, 8 Trench Midpoint	Holes 3, 6, 9 Crest Position
Time (yr)	Intact (in/yr)	100 ft long hole (in/yr)	100 ft long hole (in/yr)	100 ft long hole (in/yr)
100	0.0008	89.76	52.14	16.50
180	0.007	89.73	52.12	16.50
290	0.16	89.05	51.79	16.50
300	0.18	88.96	51.75	16.50
340	0.3	88.43	51.49	16.50
380	0.38	88.07	51.32	16.50
480	1.39	83.59	49.14	16.50
660	3.23	75.42	45.16	16.50
1100	6.82	59.48	37.41	16.50
1900	10.24	44.29	30.02	16.50
2723	11.1	40.48	28.16	16.50
3300	11.18	40.12	27.99	16.50
5700	11.3	39.59	27.73	16.50
10100	11.35	39.37	27.62	16.50

Table 5. Infiltration rates for 3.6% subsidence cases.

		Holes 1, 4, 7 End Position	Holes 2, 5, 8 Trench Midpoint	Holes 3, 6, 9 Crest Position
Time (yr)	Intact (in/yr)	184 ft long hole (in/yr)	184 ft long hole (in/yr)	184 ft long hole (in/yr)
100	0.0008	75.90	52.14	16.50
180	0.007	75.87	52.12	16.50
290	0.16	75.32	51.79	16.50
300	0.18	75.25	51.75	16.50
340	0.3	74.82	51.49	16.50
380	0.38	74.53	51.32	16.50
480	1.39	70.90	49.14	16.50
660	3.23	64.27	45.16	16.50
1100	6.82	51.35	37.41	16.50
1900	10.24	39.04	30.02	16.50
2723	11.1	35.94	28.16	16.50
3300	11.18	35.65	27.99	16.50
5700	11.3	35.22	27.73	16.50
10100	11.35	35.04	27.62	16.50

Table 6. Infiltration rates for 4.9% subsidence cases.

		Holes 1, 4, 7 End Position	Holes 2, 5, 8 Trench Midpoint	Holes 3, 6, 9 Crest Position
Time (yr)	Intact (in/yr)	252 ft long hole (in/yr)	252 ft long hole (in/yr)	252 ft long hole (in/yr)
100	0.0008	64.68	52.14	16.50
180	0.007	64.66	52.12	16.50
290	0.16	64.21	51.79	16.50
300	0.18	64.15	51.75	16.50
340	0.3	63.80	51.49	16.50
380	0.38	63.57	51.32	16.50
480	1.39	60.62	49.14	16.50
660	3.23	55.25	45.16	16.50
1100	6.82	44.77	37.41	16.50
1900	10.24	34.78	30.02	16.50
2723	11.1	32.27	28.16	16.50
3300	11.18	32.03	27.99	16.50
5700	11.3	31.68	27.73	16.50
10100	11.35	31.54	27.62	16.50

Summary of Models

Disposal Unit	Avg Depth to WT (ft)	Avg Clay Thickness (ft)	Minimum Depth to WT (ft)	Minimum Clay Thickness (ft)	Percent Subsidence	Number of Models
Slit Trench 8	75.80	11.20	75.18	11.20	2	3
Slit Trench 9	78.05	13.83			2	
Slit Trench 10	77.06	14.19			2	
Slit Trench 11	75.42	12.47			2	
Engineered Trench 4	75.18	11.46			2	
Slit Trench 1	76.32	12.68			0	
Slit Trench 2	76.59	11.29			2	
Slit Trench 3	72.93	7.70	64.31	4.09	4.9	4
Engineered Trench 3	72.14	7.13			0	
Slit Trench 4	68.61	5.70			3.6	
Slit Trench 23	64.31	4.09			2	
Slit Trench 24	61.14	1.93	55.46	1.88	2	3
Slit Trench 5	59.73	1.88			0.54	
Slit Trench 6	58.25	3.08			2	
Slit Trench 7	55.46	2.62			2	
Engineered Trench 1	57.64	16.76	55.04	15.46	0	2
Slit Trench 14	55.04	15.46			2	
Engineered Trench 5	50.80	10.19	46.12	10.19	2	3
Engineered Trench 6	46.12	10.57			2	
Slit Trench 17	49.18	13.35			2	
Slit Trench 18	48.13	12.18			2	
Slit Trench 19	49.33	13.29			2	
Slit Trench 20	48.70	12.59			2	
Slit Trench 21	49.75	12.63			2	
Slit Trench 22	49.75	12.63			2	
Engineered Trench 2	47.87	5.89			2	1
Future Plot 8-1	65.20	5.14	63.15	5.34	2	2
Future Plot 8-2	65.38	5.09			2	
Future Plot 8-3	58.86	5.79			2	

***Red text indicates corner trench

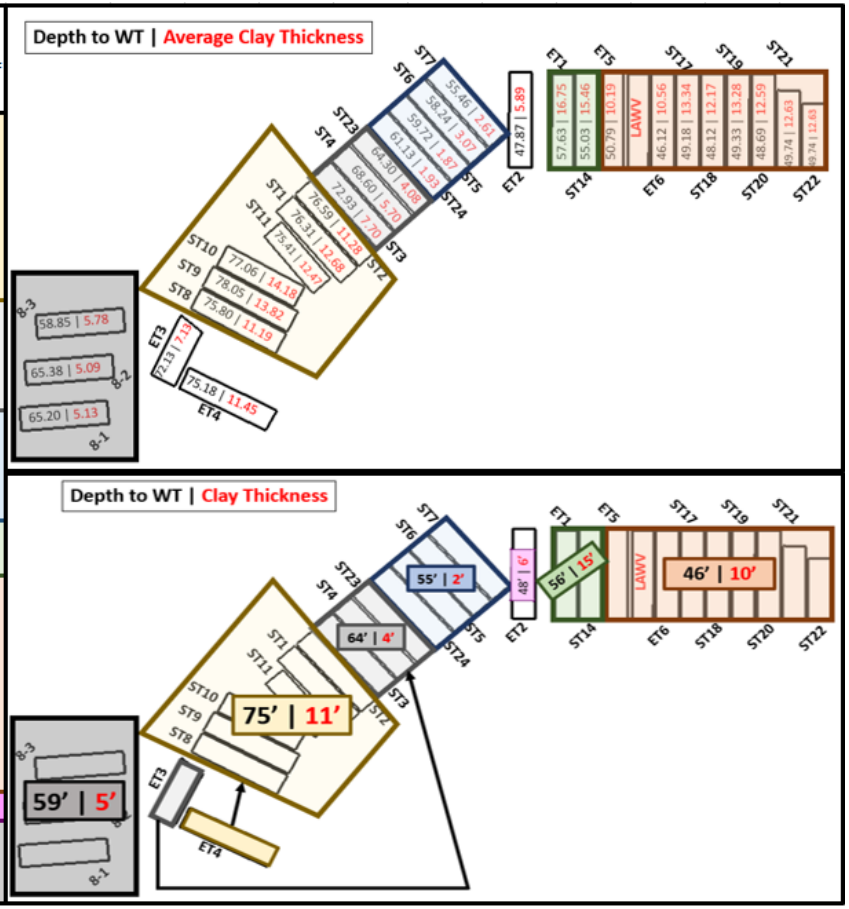

Figure 21. In total, the ELLWF PA ST/ET models will require 18 unique vadose zone models from seven unique hydro-stratigraphic groupings. Bagwell et al. reported five values for the depth to the various hydro-stratigraphic surfaces represent each of the four trench corners and the centroid of the trench. The average depth to the water table for a trench is taken as the average of these five values. The average clay thickness is taken as the sum of the thickness of upper vadose zone clayey material extending past 20 feet below ground surface (i.e., past the bottom of the disposal unit) and the thickness of the tan clay. The minimum depth to the water table and the minimum clay thickness are selected as representative of each hydro-stratigraphic grouping to maintain a reasonable degree of conservatism. The depths and thicknesses are input to PORFLOW models as rounded whole integer values.

Automated Implementation of 3D Models

An updated automated scheme has been developed and deployed for quickly implementing the various models discussed in the previous sections, while also reducing the likelihood for errors in creating PORFLOW flow and transport input files. An example case, for the hydro-stratigraphic grouping including ET5, has been implemented using this automated scheme. The material zones are shown in Figure 22 for a *YZ*-plane located in the center of the 3D model. Note that the model generically represents clayey material that falls beneath the waste zone as tan clay. Because the material properties are considered the same as the upper vadose zone, this is of no consequence, as shown in previous sections. Specific material zones are explicitly defined by specifying the grid coordinates that bound a particular material region. Overlapping of material zones has been found to lead to potential issues in PORFLOW and therefore is avoided. For example, the clayey upper vadose zone spans the *X* and *Y* coordinates of the mesh from *Z=26* to *Z=46* feet with a volume corresponding to the trench in the center of the mesh. Rather than defining all of these nodes as clayey and then overwriting with the trench material zones, a better practice is to take the union of four separate clayey regions without ever selecting the material zones corresponding to the trench. Using this methodology, the mesh can be easily transitioned from ST to ET, as necessary. The properties for these zones are extracted by the automation scheme from the files 'MaterialZones.xlsx' (specifies the material type for the zone), 'MaterialPalette.xlsx' (specifies the hydraulic properties for the material type), and 'Chemistry.xlsx' (specifies the chemical properties of the zone for each radionuclide).

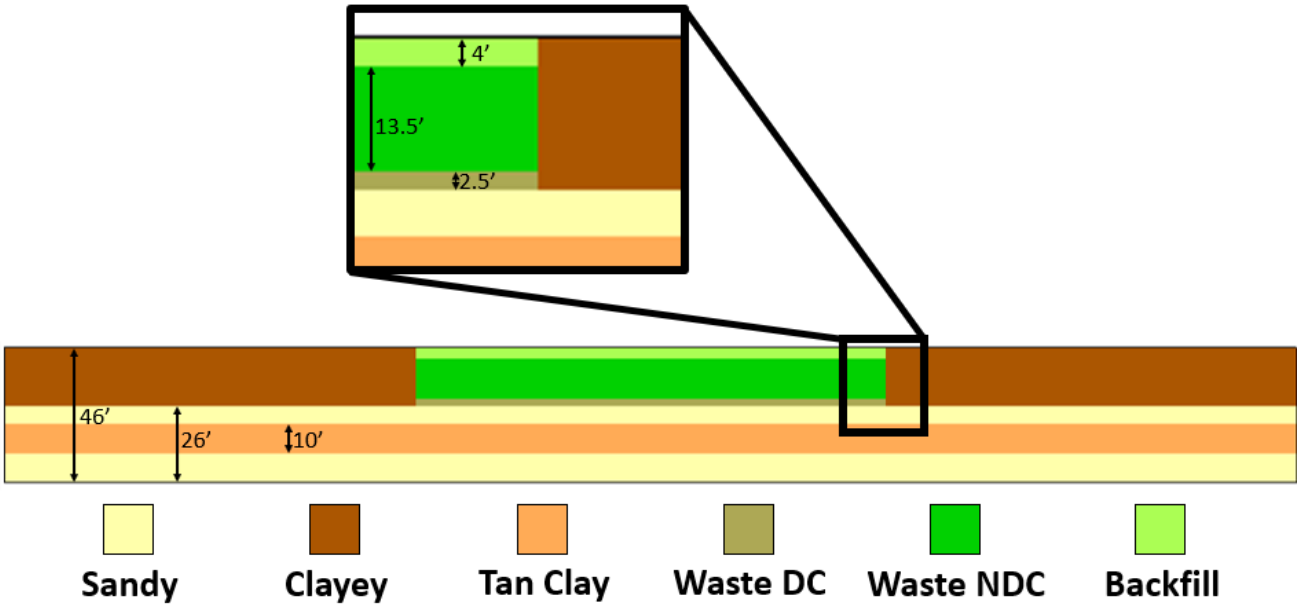

Figure 22. Material zones for hydro-stratigraphic grouping corresponding to ET5.

Timing for trench units is specified in the file 'TimePeriods.xlsx' and is based on the "Case1" timeline from Hamm et al 2018. In general, time is discretized into 74 periods each having a unique flow field that is representative of the materials present and the state of cap degradation (i.e., via water infiltration rater). All DUs that are "future units" (i.e., no waste packages placed at the start of the PA) have the same timeline. Temporal discretization may be refined if it is necessary for capturing a peak of a given radionuclide. If a unit has a different timeline than other units in its grouping, this difference is accounted

for only during a separate transport run, where steady-state flow fields are used for solving the transport equations for a given time-period.

Similar to the material properties, the infiltration zones across the top boundary of the model are explicitly specified to PORFLOW by capturing the grid coordinates that bound each region. Therefore, if it is desired to explore alternative subsidence cases, the specified grid coordinates can be changed to do so. The infiltration rate for each infiltration zone in the intact and subsidence cases are specified in the file 'BoundaryConditions.xlsx', where each infiltration rate is supplied from those in Table 3 through Table 6. No degradation occurs during the uncovered and interim closure period, and therefore, the change in infiltration occurs as a step change. To account for degradation of the final closure cap, the automation scheme interpolates the infiltration rate at the midpoint of each time period.

Notably, all other models' geometries and material zones will look similar to the example shown in Figure 22, with only the depth to the water table and the tan clay thickness updated according to those shown in Figure 21.

References

ACRi, 2018. PORFLOW User's Manual, *Keyword Commands Version 6.42.9, Revision 0*. Analytical & Computational Research, Inc., Los Angeles, CA, April 23, 2018.

Bagwell et al., 2017. L. A. Bagwell and P. L. Bennett, *Elevation of Water Table and Various Stratigraphic Surfaces beneath E Area Low Level Waste Disposal Facility*. SRNL-STI-2017-00301, Revision 1, Savannah River National Laboratory, Aiken, SC, August 2017.

Danielson, 2019a. T. L. Danielson, *Comparison of Slit Trench and Engineered Trench 3D Vadose Zone Conceptual Models*, SRNL-STI-2019-00637, Revision 0, Savannah River National Laboratory, Aiken, SC, October 2019.

Danielson, 2019b. T. L. Danielson, *A Case Study Using ST06 for Slit and Engineered Trench Model Implementation in the E-Area Low-Level Waste Facility Performance Assessment*, SRNL-STI-2019-00750, DRAFT.

Danielson, 2019c. T. L. Danielson, *A Limited-in-Scope Comparison of Subsidence Scenarios for 3D Vadose Zone PORFLOW Trench Models*, SRNL-STI-2019-00636, Revision 1, Savannah River National Laboratory, Aiken, SC, December 2019.

Danielson, 2019d. T. L. Danielson, *A Monte Carlo Rectangle Packing Algorithm for Identifying Likely Spatial Distributions of Final Closure Cap Subsidence in the E-Area Low-Level Waste Facility*, SRNL-STI-2019-00440, Revision 0, Savannah River National Laboratory, Aiken, SC, October 2019.

Dyer, 2019. J. A. Dyer, *Infiltration Data Package for the E-Area Low-Level Waste Facility Performance Assessment*, SRNL-STI-2019-00363, Revision 0, Savannah River National Laboratory, Aiken, SC, November 2019.

Hamm et al., 2018. L. L. Hamm, S. E. Aleman, T. L. Danielson, and B. T. Butcher, *Special Analysis: Impact of Updated GSA Flow Model on E-Area Low-Level Waste Facility Groundwater Performance*. SRNL-STI-2018-00624, Revision 0, Savannah River National Laboratory, Aiken, SC, December 2018.

Page Intentionally Left Blank

Distribution List

S. E. Aleman, 735-A
B. T. Butcher, 773-42A
D. A. Crowley, 773-42A
T. L. Danielson, 773-42A
K. L. Dixon, 773-42A
J. A. Dyer, 773-42A
L. L. Hamm, 735-A
N. V. Halverson, 773-42A
T. Hang, 773-42A
C. C. Herman, 773-A
J. J. Mayer, 999-W
R. L. Nichols, 773-42A
A. P. Fellinger, 773-42A
T. S. Whiteside, 773-42A
J. L. Wohlwend, 773-42A
T. N. Foster, EM File, 773-42A – Rm. 243
Records Management (EDWS)